

# Plasticity of Semicrystalline Polymers

Z. Bartczak,\* A. Galeski

**Summary:** Semi-crystalline polymers can be deformed up to a very high strain. The deformation process involves frequently a complete molecular rearrangement of the chain-folded lamellar morphology into a more or less chain-unfolded fibrillar microstructure. This transformation is likely to occur through an intermediate state of high molecular disorder at a local scale. It led to the formulation of a concept of strain-induced melting-recrystallization process as a main mechanism of the structure transformation. In contrast, several structural features occurring at moderate plastic strains are relevant to strictly crystallographic processes. The plastic deformation process of semicrystalline polymers and the micromechanisms involved are discussed. A critical discussion of experimental findings is made to point out the strength or the deficiency of the various argumentations. It is demonstrated that the crystallographic slip mechanisms, including slips: transverse and along the chains are the basic deformation mechanisms in the deformation sequence, active at all strain levels. Direct microscopic evidence of chain slip activity even at well advanced stages of the deformation process is presented. In contrary, the melting-recrystallization seems to be restricted to the high-strain stage accompanied by chain unfolding and perhaps limited to only a small fraction of the crystalline phase. In addition the experimental results demonstrates clearly that the cavitation, necessary in the Peterlin's model, is really unessential in producing high deformation and appearance of the final highly oriented structure. This can be effectively accomplished with only crystallographic mechanisms employed. A very important role in the deformation sequence is played by the partially reversible shear deformation of amorphous interlamellar layers, producing not only high orientation of amorphous component but also influencing deeply the deformation of crystalline phase, since both phases are strongly connected and must deform simultaneously and consistently.

**Keywords:** deformation; mechanisms; PE; semicrystalline polymer; yield

## Introduction

It is well recognized that semicrystalline polymers consist of lamellar crystals which are separated from each other by layers of amorphous polymer and are held together by tie molecules through the amorphous phase, see e.g.,<sup>[1]</sup>. The lamellae are formed from mostly folded chains. The thickness of lamellae is determined by the parameters

such as interfacial energies, glass transition temperature and melting temperature, undercooling, segmental diffusivity, etc. The thickness reported lies usually in a narrow range between 3 and 20 nm as obtained from observations in various types of microscopes or calculated from the long period and degree of crystallinity. It has been recognized that chain folding is not so regular as it was thought and molecular packing in lamellae is subject to considerable and irregularly distributed disorder depending on undercooling- regimes of crystallization.

Melt crystallized polymers generally exhibit a spherulitic morphology; ribbon-like

Centre of Molecular and Macromolecular Studies,  
Polish Academy of Sciences, Sienkiewicza 112, 90-363  
Lodz, Poland  
E-mail: bartczak@bilbo.cbmm.lodz.pl

crystalline lamellae are arranged radially in polycrystalline aggregates. Spherulite diameters are normally in the range of 2–20  $\mu\text{m}$ . As a spherulite is growing new lamellae are originated to fill the volume. New lamellae are added either to existing bundles of already grown lamellae or originate a new bundle. The amorphous material is incorporated evenly between lamellae in the amount corresponding to overall crystallinity. Misfit between bundle domains arising from their different shapes are filled with an amorphous material. Occasionally the lamellae may terminate; usually, however, once nucleated they continue to grow until impingement with neighboring spherulites. New lamellae are formed mostly by non-crystallographic branching.

Due to complicated, multi-level hierarchical structure of semicrystalline polymers their plastic deformation appears a complex and multistage process. Therefore, a complete quantitative description of plasticity of semicrystalline polymers requires different approaches at different scale levels of their structure: micro-, meso- and macroscopic.<sup>[2]</sup> At the microscopic level the basic micromechanisms of deformation of crystals and amorphous phase are considered. The mesoscopic level includes bending, rotations, translations and fragmentation or other structural rearrangements of lamellar stacks or mosaic blocks, deformation of spherulites, formation and multiplication of shear bands, etc. A physical interpretation of the results obtained in the macroscopic experiment (stress-strain-strain rate) is actually impossible without considering other deformation levels of smaller scale.<sup>[2]</sup>

Complex and multistage processes of plastic deformation in solid polymers involve stages that are similar to those in non-polymer materials, as e.g. generation of dislocation and their glide along the planes of crystals. However, these processes are not identical to the respective processes in non-polymer structures. Many specific features of plasticity in polymers strongly depend on their macromolecular nature.

One of the most important consequences of this nature is that both crystalline and amorphous layers co-existing in a semicrystalline polymer are intimately connected by strong covalent bonds along numerous chains crossing the crystalline-amorphous interface (tie molecules, cilia or loose non-adjacent folds entangling with other chains in the amorphous phase). Due to that it is virtually impossible to separate lamella from the adjacent amorphous layer. In fact, cavities being usually precursors of the fracture develop preferentially inside amorphous layer rather than on interfaces.<sup>[3]</sup> As a result of such strong phase connectivity, lamellae and adjacent amorphous layers can deform only simultaneously and consistently. This, in turn, induces some additional strong deformation constraints in each phase. Therefore, the mutual influence of both component's deformation each on the other can not be neglected.<sup>[4,5]</sup>

There is a number of very good published reviews on the deformation of semicrystalline polymers, see e.g.,<sup>[2,6–12]</sup> yet a clear and consistent description is still quite far away. The field is still developing and many new results were obtained in last years.<sup>[4,13–32]</sup> An excellent reviews were published recently by Oleinik.<sup>[2,11]</sup> The new results and concepts encouraged to write this report.

## Plastic Deformation of Semicrystalline Polymers

Plastic deformation of semicrystalline polymers and the mechanisms involved were a subject of intensive studies in the past decades.<sup>[2,6–11]</sup> Early studies concentrated mostly on the uniaxial tension. Later however, it has become clear that tensile deformation frequently leads to structural rearrangement that are characteristic only for this deformation mode, yet having no general significance for the interpretation of major deformation mechanisms.<sup>[2,8,9]</sup> For example, even recently it has been thought that the transition from the initial lamellar

to the final fibrillar morphology during the plastic deformation of PE or other polymers necessarily proceeds via cavitation processes in the bulk of the sample and micronecking.<sup>[33,34]</sup> However, experiments in compression and shear,<sup>[24–26,28,35]</sup> demonstrated clearly that cavitation is specific of deformation of solely uniaxial tension and is far from being a necessary condition for appearance and development of the same fibrillar morphology under other types of loading.

When a semicrystalline polymer with spherulitic morphology is loaded either in tension or compression a deviatoric stress field causes the spherulite to change shape in an affine manner at low strains (elastic range). Yielding, which begins the plastic deformation, is however, inhomogeneous within a spherulite,<sup>[36]</sup> and requires irreversible shear deformation in both the amorphous and crystalline regions. Lamellar bundles oriented at 45° to the principal stress direction experience the largest resolved shear stress, begin to deform by interlamellar shear (stretching of the amorphous regions between crystals) and/or intracrystalline shear (sliding polymer chains along planes containing the covalently bonded molecular axis). Deformation continues until the original spherulites are destroyed and transformed to well oriented microfibrils with transverse dimensions of the order of 10 nm.<sup>[33]</sup> Large-strain plastic deformation causes the chain axis to orient preferentially in the principal stretch direction.

Due to complex, hierarchical structure and morphology the process of plastic deformation of semicrystalline polymer is also complex and multistage. The deformation mechanisms are quite complicated and can diverse at the local scale depending on the local morphology, which additionally is modified substantially with increasing strain by the proceeding deformation. Due to structure and morphology evolution the deformation sequence consists of several stages, involving various micromechanisms, many of which being identified to be similar to those known in non-polymer materials.

The identified basic micromechanisms of deformation of a semicrystalline polymers include crystallographic mechanism, like crystallographic slip, mechanical twinning or martensitic transformations (stress-induced phase transformations), all active in the crystalline phase. These mechanisms are supported by interlamellar shear, lamella separation and stack rotations, all operating in the amorphous phase. These mechanisms are engaged in a complex deformation sequence in which particular mechanisms are activated and terminated at various strains. Several models were formulated to describe the full deformation path. Three most important models: the Peterlin's micronecking model,<sup>[33,34]</sup> the melting–recrystallization model,<sup>[37,38]</sup> and the crystallographic model,<sup>[6,8,9,16,35,39]</sup> will be discussed in the succeeding sections of this paper.

## Deformation of Polymer Crystals

Taking into consideration the yield behavior of semicrystalline polymers there are two conflicting approaches concerning crystals. The first presumes that the process of deformation is composed of a simultaneous melting and recrystallization of polymer under adiabatic conditions,<sup>[37,38]</sup> and as less relevant will be discussed later. The second, so-called crystallographic approach,<sup>[6,39]</sup> uses the idea derived from the classical theory of crystal plasticity. Bowden and Young in their review published in 1974,<sup>[6]</sup> considered in detail the classical crystallographic (nonpolymer) mechanisms of plasticity in polymer crystals, and convincingly demonstrated, that the picture based on classical concepts of nucleation of dislocations and their glide along the crystal lattice agrees well with the behavior of semicrystalline polymers. This approach was further developed by Young and other researchers,<sup>[6,8,9,16,35,39]</sup>. A vast experimental evidence, primarily X-ray data,<sup>[24,40–43]</sup> demonstrated clearly that the deformation of polymer crystals proceeds according to the crystallographic mechanisms, indeed.

The plastic deformation of polymer crystals, like the plastic deformation of crystals of other materials, is generally crystallographic in nature and takes place without destroying the crystalline order. The only exception to this is a very large tensile deformation, when cavitation and voiding lead to unravelling the folded chains and break down completely the crystals; new crystals may form then with no specific crystallographic relationship with the original structure.<sup>[18,44]</sup> Polymer crystals can deform plastically by crystallographic slip, by twinning and by martensitic transformation. Among these the slip mechanism is the most important one since it can accommodate plastic strains much larger than the other two mechanisms. The crystallographic slip consist of sliding of blocks of a crystal one over another along define crystallographic plane (*slip plane*) in the define direction within this plane (*slip direction*), as shown in Figure 1. The geometry of the slip is described by so-called *slip system*. The notation for the slip system is  $(hkl)[uvw]$  where  $(hkl)$  denote the

slip plane while  $[uvw]$  is the slip direction ( $h,k,l,u,v,w$  are the Miller indices).

The slippage of crystals is not uniform and is essentially anisotropic: slips along some planes (easy slip planes) are much easier than along others. Generally the easy slip planes are those of the closest packing, i.e. of large interplanar distance. In most cases the slip direction coincides with the direction of the closest packing in the slip plane. To preserve the crystal structure after a deformation, the unit vector of displacement (slip) must be equal to the lattice translation vector. Crystallographic slips are not processes occurring simultaneously over the whole crystallographic plane. They are produced by the glide of a linear defect or dislocation along the slip plane. Screw and line dislocations play a great role in activation and propagation of a slip.

The slip begins when the shear stress in the slip direction,  $\tau$  reaches a certain level that is critical for the given slip system,  $\tau_0$ . Such a stress is referred to as the *critical resolved shear stress*. For uniaxial tension or compression under an applied stress  $\sigma$  the resolved shear stress for a given slip system is given by,<sup>[45]</sup>

$$\tau = \sigma \cos \chi \cos \lambda$$

where  $\chi$  and  $\lambda$  are the angles of the slip plane normal and of the slip direction with respect to the axial stress  $\sigma$ , respectively (cf. Figure 1). Yielding, i.e. the beginning of plastic deformation, starts when the critical resolved shear stress is reached in any family of planes with low  $\tau_0$ . This can be accomplished by either an increase of the axial stress or a decrease of the Schmid factor,  $\cos \chi \cos \lambda$ , by plane tilting with respect to the axial stress. Therefore, the oblique orientation of chains with respect to the stress is advantageous for activation of slip and to achieve plastic yielding at a lower energy cost. In contrary to low molecular crystals the critical resolved shear stress in polymer crystals shows usually a significant dependence on the stress normal to the shear plane (or pressure).<sup>[2,24,43,46–48]</sup> Critical resolved

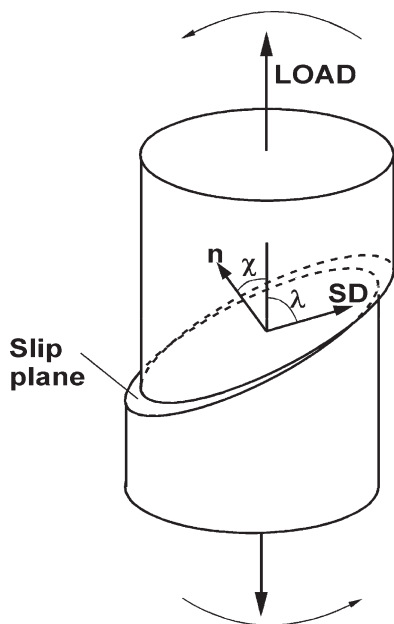


**Figure 1.**

Definition of a slip system: slip plane and slip direction (SD). Drawn after Ref. [6]

shear stresses of main active slip systems were estimated for crystals of PE,<sup>[24,49,50]</sup> Nylon-6,<sup>[46]</sup> and iPP,<sup>[50–52]</sup>

When a single slip system operates along a single plane between two crystal parts, both of these parts adjust themselves to the tensile (or compressive) axis - the crystal experiencing shear rotates with respect to the loading axis. One part of the crystal shifts with respect to the other one in such a way that the structural disturbances would be minimized and the crystal structure after the shear would be restored at the smallest possible distance from the dislocation core.<sup>[6,8]</sup> Slip geometry implies that crystal undergoing single slip rotates relative to the stress axis (Figure 2), always toward the direction of the maximum tension.<sup>[6]</sup> In the case of uniaxial tension, the rotation goes in the direction of the tensile axis; in the case of uniaxial compression, the rotation is directed away from the compression axis. Observing such rotations, one can obtain information on the deformation micromechanisms involved,<sup>[6,8,9,24]</sup> even at the very local microscale.

Crystallographic slip processes in polymer crystals demonstrate several features unique to polymers and reflecting their macromolecular structure. The most important one is the restriction imposed by chain structure for the choice of slip planes. As crystallographic processes can

not lead to chain ruptures and lattice symmetry remains intact, the dislocation glide is possible only along planes that are parallel to the chain axis. For polymer crystals, the most typical modes of slip are the chain slip and transverse slip: the former realized by the glide along direction of the chain axis, while the latter by the glide in direction perpendicular to it, both in the same plane containing chain axis, as illustrated in Figure 3. For example, studies on highly oriented polyethylene revealed that the (100)[001] chain slip and the (100)[010] transverse slip, both operating in the (100) plane are the easiest slip systems in orthorhombic PE crystals.<sup>[24]</sup>

As polymer crystals exhibit usually the folded structure these folds impose another limitation on the development of crystallographic deformation processes,<sup>[54]</sup> folds should not be destroyed during deformation. For this reason slip is preferred in planes containing chain folds. Additionally, in crystals like PE, as glide of dislocation is realized by motion of twist defects, generation of such defects is easier for loose folds, i.e. in crystals of low perfection.<sup>[55]</sup>

The slip in lamellae of polyethylene and other polymers can proceed in two different ways: in the form of fine (homogeneous) or coarse (heterogeneous, block) slip.<sup>[2,6,9]</sup> In fine slip, displacement by one, or more, lattice vectors occurs practically on every

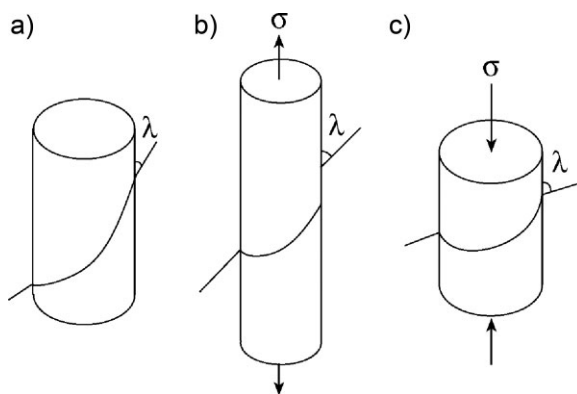


**Figure 2.**

Rotations of a single crystal undergoing a slip in a single system, 6,8,9: (a) initial crystal, (b) crystal after uniaxial tension ( $\lambda$  decreases), and (c) crystal after uniaxial compression ( $\lambda$  increases).  $\lambda$  is the angle between the slip direction and the axis of the stress. Drawn after Ref. [6]

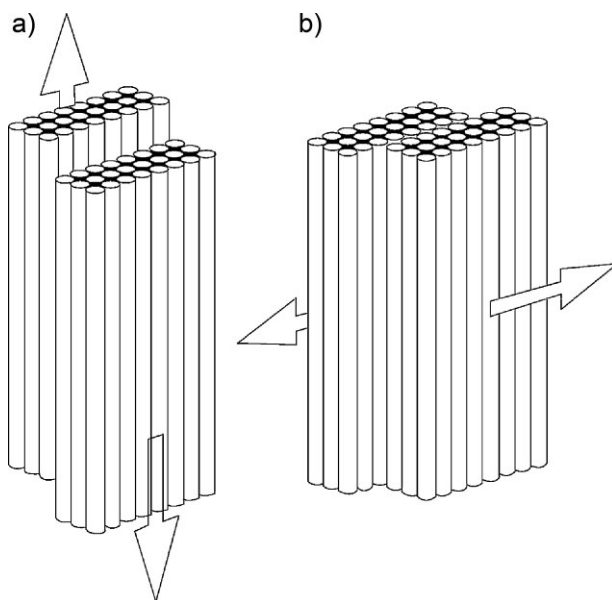


**Figure 3.**

Two types of crystallographic slip in macromolecular crystals: (a) chain slip (longitudinal) and (b) transverse slip. Arrows denote the direction of the chain translation, Drawn after Ref. [53].

other lattice plane in the crystal, as illustrated in Figure 4. This type of slip leads to a change in the angle between the chain axis and the normal to the lamellar surface, i.e. to a gradual tilting of chains in the crystallite with advancing shear strain. Consequently, the lamellae become progressively thinner as homogeneous fine slip advances. In the case of coarse slip, significant shear displacements appear only along a few neighboring crystal planes, so that the slip resembles sliding the crystal blocks one past another. The coarse slip

results from heterogeneous nucleation of dislocations, caused for example by defects already present in lamella or by local stress concentrations appearing on lamella face. Coarse slip takes place in lamellae which are highly defected or have block sub-structure and also in the late stages of deformation, when the crystals are already thinned due to advanced fine slip and become prone to slip instabilities,<sup>[35]</sup> while the stress concentrations may arise from taut tie-molecules. As the blocks between localized slip zones are relatively large, the angle between the

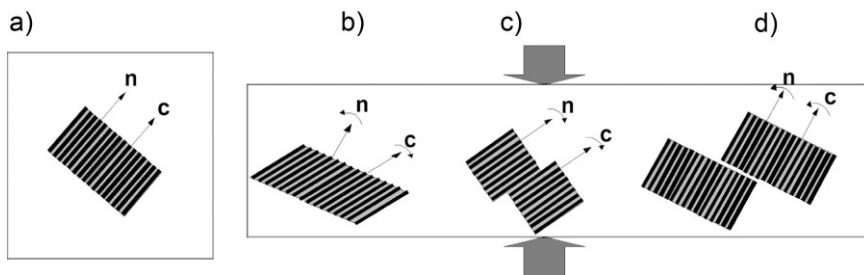


**Figure 4.**

Rotation of the chain axis,  $c$  and lamella normal,  $n$  produced by fine chain slip (b), coarse chain slip (c), interlamellar shear (d). In (a) orientation of both vectors in lamella prior to deformation is shown. Gray arrows indicate direction of compression.



chain axis and the normal to the crystal surface does not change during the deformation, i.e. no chain tilting takes place. Thickness of the blocks in lamellae deformed by the heterogeneous (block) slip does not change, too. Highly advanced coarse slip results in plastic instabilities and can lead eventually to fragmentation of lamellae (*cf.* Figure 5).

Figure 4 illustrates the rotations of the chain direction, **c** and the normal to lamellar surface, **n** resulting from fine and coarse slip. Additionally, rotations related to the interlamellar shear, discussed in the next section, are also shown. These rotations are similar in tensile and compressive deformation and can be summarized as follows:

- fine chain slip – **c** rotates towards the direction of maximum extension (i.e. the loading direction in the case of tension or direction perpendicular to loading direction in compression), **n** rotates in opposite direction, away of it.
- coarse slip- both **c** and **n** rotate together towards the direction of a maximum extension.
- interlamellar shear - **c** and **n** rotate together away of the direction of a maximum extension.

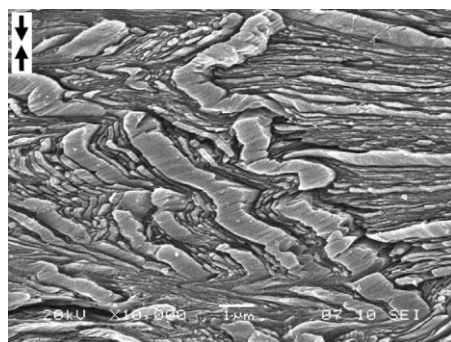


**Figure 5.**

Scanning electron micrograph of the etched surface of a high pressure crystallized PE after compressive deformation at a compression ratio  $CR \approx 3$ . Fine and coarse slip, leading to kinks and fragmentation can be seen. Direction of compression indicated with arrows.

Monitoring of these specific rotations of **c** and **n** vectors with X-ray scattering techniques allows not only to detect easily an activity of crystallographic slip or interlamellar shear but also to differentiate precisely fine and coarse slips.<sup>[6,8,9,24]</sup> Combination of WAXS and 2-dimensional SAXS proved to be one of the most powerful tools for probing the crystal slip processes. 2-D WAXS and 2-D SAXS patterns reveal the preferred orientation of the chain axis, **c** and lamella normal, **n**, respectively. X-ray experiments done for several polymers deformed in uniaxial tension, uniaxial or plane-strain compression and simple shear confirmed the crystallographic slip mechanisms as the major active deformation micromechanisms in semicrystalline polymers.<sup>[6,46,56–60]</sup> The fine slip was found predominant mode in many polymers, including PE, at room temperature and low or moderate strains, especially under compression.<sup>[6,8,9,24,25,28,35]</sup> Fine slip is also a main slip mode in deformation of oriented PE, PET, Nylon-6 and PTFE under both compression and tension. The coarse slip is more frequent in tensile deformation and competes with fine slip. Its role usually increases with the increasing total strain of the sample, in all deformation modes.<sup>[19,28,30,31]</sup> Several examples of identification slip systems operating in samples of textured PE can be found in.<sup>[24]</sup> In this work rotations of the chain axis was monitored precisely with WAXS pole figures, while rotations of lamella normal was traced with 2-D SAXS.

Plasticity of polymer crystals, as any other crystals, should satisfy several conditions. As it is known,<sup>[61]</sup> no deficient plastic deformation of a crystal of any orientation requires five independent slip systems. However, the limitations due to the covalent nature of chain bonding and usual low symmetry in polymer crystals allow only for at most three independent slip systems.<sup>[2,11,24]</sup> This means that the strain cannot be fully accommodated in polymer crystals. It is this deficit of slip that leads to violation of integrity and nucleation of microcracks in the regions with limited

glide freedom;<sup>[44]</sup> as a result, polymer single crystals appear brittle. However, two additional glide systems that are necessary for the complete strain accommodation can be provided by their adjacent amorphous phase. Interlamellar shear in the plane roughly perpendicular to the chain axis effectively substitutes the lacking slip systems in polymer crystals. Therefore, the full strain accommodation in plastic deformation is possible only in semicrystalline polymers, which in fact appear highly ductile. Another possibility to overcome the deficiency of deformation in spite of a limited number of possible slip systems is a slippage of the mosaic block within lamellae (by two orthogonal coarse slips), postulated by Strobl et al.<sup>[19,20]</sup> Such a block slippage might substitute two lacking independent glide systems similarly to interlamellar shear.

Along with slip two additional crystallographic mechanisms of deformation, twinning and stress-induced martensitic phase transformation have been shown to occur in the early stages of plastic deformation of PE.<sup>[56,62-68]</sup> Similar mechanisms were also found active in several other polymers. These two deformation modes are important mechanisms since they result in plastic deformation even if slip is geometrically unfavorable and in this way become supplementary to slip systems. Although both twinning and martensitic transformation accommodate much less strain than any slip process, they frequently appear necessary in the deformation sequence because they lead to a drastic reorientation of the lattice, which in turn, may restore favorable geometrical conditions for the slip. The critical shear stresses for twinning and martensitic transformation in the *a-b* plane are lower than that for slip in that plane,<sup>[24,69]</sup> and only little higher than for the easiest slip system.

The chain nature of polymer molecules again determines that all twinning and martensitic transformations will produce shear strains only transverse to the chain direction. A theoretical geometrical

framework for predicting modes of twinning and martensitic transformations in PE crystals has been established by Bevis and Crellin.<sup>[70]</sup>

## Dislocations in Crystal Plasticity

The overwhelming evidence accumulated over several decades is that the crystalline lamellae of polymers, much like all crystalline ductile metals, deform plastically by the generation and motion of crystal dislocations. Screw dislocations are of primary importance, even though the role of edge dislocations is also evident.<sup>[9]</sup> Crystallization of any substance is always easier, if screw dislocations are engaged, due to a dihedral angle benefit. The observed density of pre-existing dislocations varies widely on different specimens and different low molecular weight materials, ranging from a few to  $\sim 10^4/\text{cm}^2$ . Crystallization of polymers is also prompted by screw dislocations. Screw dislocation growth mechanism in polymers was reported since a long time,<sup>[71,72]</sup> in polymer single crystals. The estimate of the number of existing dislocations in polymer crystals is few orders of magnitude larger than in low molecular substances,  $10^5$ – $10^8/\text{cm}^2$ .<sup>[73]</sup> Dislocations in deformed PE were directly observed,<sup>[74-76]</sup> It was shown,<sup>[76]</sup> that they concentrate in PE in easy slip planes and determine the shear deformation of the sample in the [001] direction. Screw dislocations were also observed by dark-field electron microscopy in single crystal PE during its deformation.<sup>[71]</sup> The macroscopic behavior of PE ( $\sigma$ - $\epsilon$  curves) was subsequently described in a number of publications within the framework of models with screw dislocations, see e.g. Ref.<sup>[9]</sup>

The amount of mobile dislocations that is present in polymer crystal is sufficient to initiate its plastic deformation. However, during crystallographic slip many more new screw dislocations must be generated at crystal edges and propagate through the crystal in order to accommodate for plastic flow. This process of emission of



dislocations from the edges of the lamellae across the narrow faces that was initially proposed by Peterson,<sup>[77,78]</sup> explored further by Shadrake and Guiu,<sup>[79]</sup> and more rigorously by Young,<sup>[39,80]</sup> is now widely accepted.

The model of thermal nucleation of screw dislocations from Peterson,<sup>[77,78]</sup> and Young,<sup>[39,80]</sup> has been shown to account fairly well for the plastic behavior of PE,<sup>[81,82]</sup> and PP,<sup>[83]</sup> and for the yield stress dependency on crystal thickness. Elastic line energy calculations indicate that nucleation of screw dislocations is more favorable than that of edge dislocations.<sup>[79,84]</sup> Glide is also easier for the former,<sup>[85]</sup> It has been shown that screw dislocations parallel to the chain stems may be nucleated from the lateral surface of thin polymer crystal platelets upon coupled thermal and stress activation.<sup>[77,78,86]</sup>

The activation volume of dislocation emission was determined from strain rate jump experiments during uniaxial compression of polyethylene.<sup>[87]</sup> The mean level of activation volumes were of the order of 350 of crystallographic unit cells and the estimated typical radius of the dislocation was 3.8 nm, i.e. much smaller than the usual lamella thickness (ca. 20 nm).<sup>[88]</sup> The Burgers vector of such dislocation must be short, few lattice units only. Apparently the dislocations of such characteristics are the easiest to generate. It is then logical to assume similar values for the activity area of screw dislocations arising during melt crystallization.

The magnitude of the shear stress needed to move a dislocation along the slip plane was first determined by Peierls,<sup>[89]</sup> and Nabarro.<sup>[90]</sup> For orthorhombic unit cell of a crystal it varies exponentially with the ratio of both unit cell axes perpendicular to the macromolecular chain direction. For a (100) plane being the closed-packed plane (**a** axis larger than **b** axis) the critical resolved shear stress reaches the minimum. That is because for closed-packed planes the interplanar bonds are weaker which results in lower activation energy and lower shear stress. The result is

that the dislocations tend to move in the closest packed planes and in the closest packed direction since the Peierls-Nabarro force is smaller for dislocations with short Burgers vector.

Similarly to low molecular crystals, the factors limiting the deformation can be either the nucleation rate of dislocations or the lattice resistance to their glide (the Peierls barriers, lattice defects). For example, the nucleation of screw dislocations on the lamellar surface controls the plasticity rate in PE<sup>[39]</sup> while in quasi-single crystals of Nylon-6, dislocation glide turns out to be the mechanism that controls the overall rate of plasticity.<sup>[43,91]</sup> The existing data suggest however, that in most cases, the kinetics of plasticity in polymer crystals is controlled by the nucleation of dislocations.

## Generation of Dislocations

There was a question whether the rate controlling process in plastic flow of semi-crystalline polymers is nucleation of dislocation or their mobility. The answer must indicate nucleation because the number of incorporated pre-existing dislocations is rather insufficient to allow for an undisturbed slip. The dislocations must be continually injected from the interfaces to keep the slip alive.

As the mechanisms of dislocation propagation is widely accepted for slip mechanisms in semicrystalline polymers there are uncertainties about how the dislocations are generated. The density of dislocation in polymer crystals is estimated at the level from  $10^5$  to  $10^8/\text{cm}^2$ .<sup>[92]</sup> This number is not sufficient to give rise to a fine slip most often observed during polymer plastic deformation. There must be an efficient way of generation of new dislocation in crystals. In metals and other large crystals the identified source of dislocations is a multiplication mechanism known as Frank-Read source.<sup>[62]</sup> The Frank-Read mechanisms involves a dislocation line locked on both ends. When the shear stress is applied above a certain critical value the

dislocation line will bow to form first a semicircle and then the line spirals around the two immobilized ends, forming finally the dislocation ring which will continue to grow and move outward under the applied stress. At the same time the original dislocation line has been regenerating and is ready to repeat the whole process. In this way a series of dislocation rings is generated indefinitely. In polymer crystals this elegant process can not be active because the crystals are usually too thin for the dislocation line to spiral up and to form a dislocation loop.

Theoretical calculations predicted,<sup>[79]</sup> and experiments confirmed,<sup>[6]</sup> that polyethylene lamellae deform easily by slip in the direction of *c*-axis. Shadrake and Guiu,<sup>[79]</sup> pointed out that in the case of PE the energy necessary for creation a screw dislocation with the Burgers vector parallel to chain direction can be supplied by thermal fluctuations. It was shown that the change in the Gibbs free energy,  $\Delta G$ , associated with creation of such dislocation under the applied shear stress,  $\tau$  (ie. the energy which must be supplied by thermal fluctuations) is equal to:

$$\Delta G = \frac{Kb^2l}{2\pi} \ln\left(\frac{r}{r_0}\right) - \tau b l r,$$

where  $l$  is the stem length;  $b$  is the length of the Burgers vector;  $K$  is the shear modulus of a crystal;  $r$  is the radius of dislocations (the distance from dislocation line to the edge of lamellae); and  $r_0$  is the core radius of dislocations.

There are still doubts whether the model can be applied over the entire range of temperature, i.e. from the temperature of glass transition to the onset of melting process. The dispute concerns the upper temperature of validity of this approach. Crist,<sup>[93]</sup> suggested that the temperature of  $\gamma$  and  $\alpha$  relaxation processes of PE are the limits of applicability of the model. Young,<sup>[86]</sup> and Darras and Seguela,<sup>[82]</sup> have used that approach to model the yield behavior of bulk crystallized and annealed polyethylene at a much higher temperature. Brooks et al.<sup>[94]</sup> reported the existence of a

transition in the range from  $-60^\circ\text{C}$  to  $20^\circ\text{C}$ , depending on the material and strain rate, above which the Young's model can not be applied. They pointed out that there is a relationship between the transition temperature and  $\beta$ -relaxation and suggested that below the transition temperature the yield process is nucleation controlled, while above it becomes propagation controlled. However, Galeski et al.<sup>[35]</sup> have shown that in plane strain compression for HDPE at  $80^\circ\text{C}$  yielding is mainly associated with (100) fine chain slip within crystalline lamellae. Moreover, it was shown that for linear polyethylene only fine slip occurs up to the deformation ratio of 3, associated with chain tilt and thinning of lamellae. Only at higher deformation the widespread fragmentation of those significantly thinned (even up to one third) lamellae by coarse slip takes place. That is because further thinning by fine slip becomes unstable - much like layered heterogeneous liquids responds by capillary waves and breakup of stacks of layers.<sup>[35]</sup>

Seguela,<sup>[95]</sup> proposed that the driving force for the nucleation and propagation of screw dislocations across the PE crystal width relies on chain twist defects that migrate along the chains stems and allow a step-by-step translation of the stems through the crystal thickness. The motion of such thermally activated defects is responsible for  $\alpha$  crystalline relaxation.

In contrast, in coarse grained polycrystalline metals the rate mechanism of deformation is governed almost exclusively by either the intrinsic lattice resistance or the resistance of localized obstacles to dislocation motion. Dislocation nucleation in crystal plasticity as a rate controlling process is found only in nearly perfect crystals or in polycrystals in the nanoscale range.

In PE and similar semi-crystalline polymers the preferred systems are those of chain slip in planes of the largest interplanar separation: (100) in PE; (001) in nylon-6. In such systems, because of the very high longitudinal stiffness of the chain molecules the screw dislocations with much

narrower core can be expected to be the most likely carriers of plasticity associated with the rate mechanism. That hypothesis was confirmed indirectly by Peterman and Gleiter,<sup>[75]</sup> who made the first TEM observations of screw dislocations in PE lamellae. For the reason that the lamellae thicknesses are only in the nanoscale range (10–20 nm) it has been suspected for a long time that the rate controlling process must be the emission of dislocations from lamellar edges under stress with the already nucleated dislocations exiting rapidly the lamellae on the other side. This requires the process to be repeated continuously. This scenario was re-examined in 2000 by Brooks and Mukhtar,<sup>[96]</sup> Kazmierczak et al.<sup>[87]</sup> studied deformation of PE samples with lamella up to 170 nm thick, i.e. much above the usual 10–20 nm thickness range. It turned out that when lamella thickness exceeds 28 nm the mechanism of emission of screw dislocation lines from lamella edges must be superseded by another, more ubiquitous one that is no longer sensitive to lamella thickness.

In examining new possibilities for the description of dislocation emission in PE crystals the recently developed fundamental considerations by Xu et al.<sup>[97–100]</sup> were revisited. In the consideration of the rate mechanism of plastic flow in individual lamellae the attention was limited to deformations resulting from shear on the (100) [001] system as it dominates over all others. The principal local plastic deformation process is then  $\gamma_{13}$  shear, promoted by the resolved  $\tau_{13}$  shear stresses, referred to the PE orthorhombic crystal structure, based on the well established slip on the (100)[001] crystallographic system.<sup>[4,101,102]</sup>

Figure 6 depicts three modes of dislocation nucleation-controlled processes of chain slip possible on the (100) [001] system. The process identified as A is that considered earlier nucleation of a fully formed screw monolithic dislocation from the narrow face. Clearly, as the lamella thickness  $l$  increases the ever increasing activation energy of this mode will no longer be kinetically possible. Thus, two

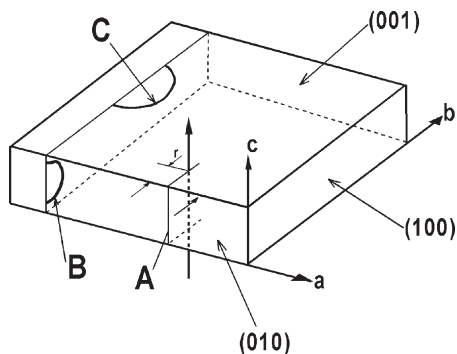


**Figure 6.**

Sketch depicting a geometry of a typical lamella showing the principal chain slip system (100)[001] and the three separate modes of dislocation nucleation: A monolithic screw, B screw loop and C edge loop. Drawn after Ref. [88].

other modes were considered: a screw dislocation half loop nucleation, still from the narrow face, and an alternative process of edge dislocation half loop nucleation from the wide face of lamellae, depicted as processes B and C, respectively, in Figure 6.

The energetics of all three processes has been considered rigorously by Xu and Zhang,<sup>[99,100]</sup> based on a variational boundary integral approach. Argon et al.<sup>[88]</sup> reconsidered critically the previous developments of screw dislocation emission monolithically from edges of thin lamellae (process A). It was shown that after elimination of several questionable assumptions the previously proposed model of screw dislocation emission from lamella edges can provide results as accurate as the more rigorous developments of Xu. The obtained equations are essentially similar to the formulas derived by Shadrake and Guir,<sup>[79]</sup> although the fundamental parameters are expressed in terms of shear strength of the slip system in exchange to two parameters: the radius of dislocations and their core radius. Both show a linear dependence of  $\Delta G$  on lamellae thickness.

The two other alternative dislocation sources, B and C, for which the lamella thickness plays no role were also considered by Argon et al.<sup>[88]</sup> This led to

the expressions not involving lamellae thickness at all.

The comparison of the compressive yield stress calculated for all three mechanisms with experimental data of Kazmierczak et al.<sup>[87]</sup> is shown in Figure 7. The data points for thin lamellae are close to the prediction of the model of monolithic screw dislocations. The plot suggest a sharp departure from the mode of screw dislocation line nucleation to the half loop modes roughly around 16 nm of lamella thickness. The experiments show a more gradual transition at a lamella thickness of roughly 28 nm. For lamellae thicker than 28 nm the data points fall in between the models for nucleation of edge half loops and screw half loops.

The results of experiments by Kazmierczak, et al.<sup>[87]</sup> with PE samples containing very thick lamellae prompted a re-examination of the Young's model, recently considered again by Brooks and Mukhtar,<sup>[96]</sup> that also other alternatives that must be taken over for thicker lamellae. These two newly described dislocation sources, no longer dependent on lamellae thickness have explained well the leveling off the plastic resistance for lamellae thicker than approx. 28 nm. Additionally the new approach offers much better agreement with the published

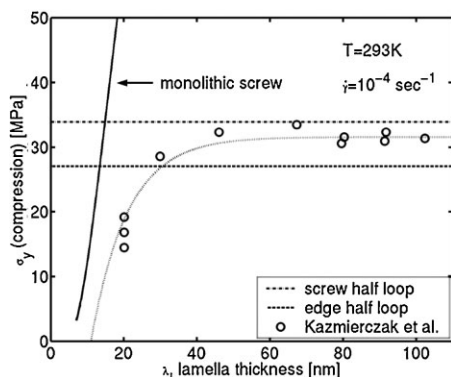


**Figure 7.**

Dependence of compressive flow stress of polyethylene at 293 K and  $\gamma=1$  on lamella thickness: compared with three theoretical models, 87,88. Reproduced from the Ref. [88] with permission of Elsevier © 2005.

dependencies of the plastic resistance of PE on temperature, as compared to the model of Young. It also predicts the activation volumes, which agree quite well with those estimated experimentally.

The dependencies of tensile resistances on temperature calculated for the mode of monolithic screw dislocation emission from lamella edges and those of edge and screw half loop emissions from the large and small faces of the lamellae, respectively, are plotted in Figure 8. The experimental data points of Brooks and Mukhtar,<sup>[96]</sup> lie along a line that parallels the half loop nucleation modes and far from the prediction of the usually considered mode of nucleation of monolithic screw dislocations. However, their positions are considerably below the models of the half loop nucleation. The discrepancy is partly due to the relatively low level of crystallinity of  $\sim 0.538$ . If the data were converted to account a crystallinity of 0.9 the experimental points would move up to the dotted curve lying much closer to the model of nucleation of edge dislocation half loops. The predictions of Figure 8 can suggest that the flow stress for thinner lamellae might be governed by the

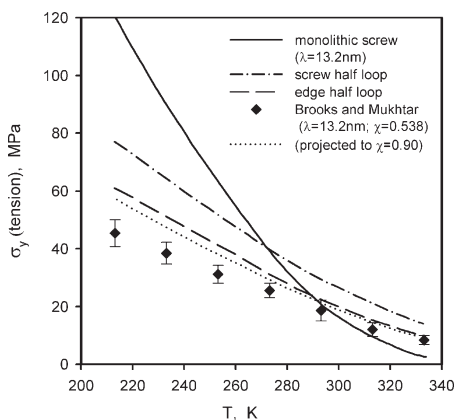


**Figure 8.**

Predictions of modes A, B and C models of dislocation nucleations for the temperature dependence of the tensile yield stress of polyethylene and compared with experimental results of Brooks and Mukhtar,<sup>[96]</sup> for their PE2 material of moderate level of crystallinity at  $X = 0.538$ . Dotted line projects experimental results for  $X = 0.9$ . Reproduced from the Ref. [88], with permission of Elsevier, © 2005.

mechanism of monolithic emissions of screw dislocations at higher deformation temperatures and the mechanism could switch over to that of half loop nucleation at lower temperatures.

### Deformation of Amorphous Component and its Role in the Plastic Deformation Sequence

There are three recognized main modes of deformation of the amorphous material in semicrystalline polymers: interlamellar slip (shear), interlamellar separation and lamellae stack rotation,<sup>[6,8]</sup> illustrated in Figure 9. Interlamellar slip (Fig. 9a) involves shear of the lamellae parallel to each other with the amorphous layer undergoing shear. It is a relatively easy mechanism of deformation for the material above  $T_g$ . As shown in Figure 4 interlamellar shear produces rotation of both chain direction and lamella normal away of the direction of maximum extension, which allows identification of this deformation mode. Using X-ray scattering it was possible to show that interlamellar slip is an important mechanism during deformation of PE. Keller et al.<sup>[103–105]</sup> found that interlamellar slip occurred during drawing, rolling and annealing LDPE both at and above room temperature and suggested it was the principal deformation mechanism above 80 °C.<sup>[105]</sup> The occurrence of interlamellar shear in

other polymers was widely reported.<sup>[2,6,8,9,12]</sup> It was established that the recoverable part of deformation can be almost entirely attributed to the reversible interlamellar slip.<sup>[19,20,23,29,31,43]</sup> This is due to the structure of the amorphous component constituting a molecular network of entangled chains closely connected to the adjacent crystalline lamellae through tie molecules. Such a network should demonstrate the hyperelastic rubber-like behavior. As the entangled chains and tie-molecules connecting crystals become extended on deformation, they tend to pull the crystals back to their original positions when the sample is unloaded.

Interlamellar separation (Figure 9b) is induced by a tensile stress component perpendicular to the lamellar surface.<sup>[105]</sup> It is responsible for thickening of intercrystalline layers in a sample and an increase of the long period in the direction of tension. As the amorphous phase behaves like a perfect rubber, this type of deformation should be difficult since a change in the lamellae separation should be accompanied by a transverse contraction, which is however, hindered by lateral constraints imposed by crystalline lamella on the amorphous layers, so that the deformation must involve a change in volume. Since rubbers generally have high bulk modulus and relative low shear modulus, they are usually resistant to volume changes (the Poisson ratio = 0.5). This is frequently a source of the cavitation within amorphous layer between lamellar

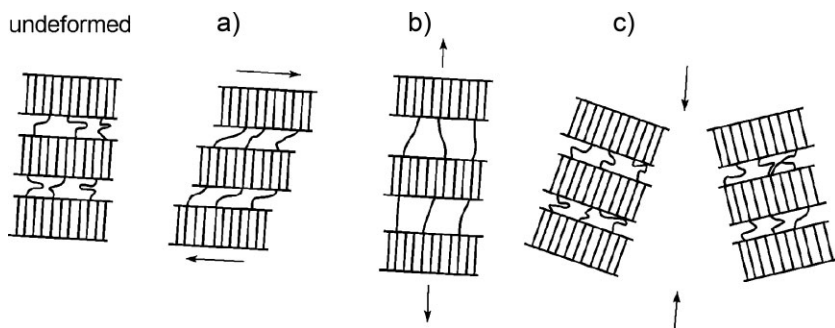


**Figure 9.**

Deformation modes of the amorphous phase: (a) interlamellar slip (shear), (b) interlamellar separation, (c) stack rotation. Drawn after Ref. [6].

crystals.<sup>[2,12,106]</sup> The deformation resistance to interlamellar separation depends on the amount of active tie-chains and on their length distribution, as well as on the transverse size of crystallites. Two mechanisms are possible for the implementation of this deformation mode: either cavitation, leading to the formation of voids or crazes, or plastic flow of the amorphous material into structural traps,<sup>[2,9]</sup> like sites with a poor chain packing. The flow into such traps is preferable in structures with thin and narrow lamellae, which allow a lateral compression of the amorphous layer along the interfaces during a deformation. However, such a compression is much constrained in a structure with wide lamellae, which favours the separation mode with the appearance of cavitation. However, cavitation increases the deformation resistance of interlamellar separation, as a new interface must be created. A cavitation-free flow of the amorphous material, surrounding the lamellae, into structural traps is frequently impeded since ruptures of tie-chains may be necessary in this case. Therefore, the most likely mechanism, which facilitates cavitation-free processes and thus reduction of the deformation resistance of the amorphous layer, is the cooperative bending of lamellae (kinking) between local bridges of tie-molecules.<sup>[107,108]</sup>

When the lamellae arranged in stacks are embedded in the amorphous matrix then these stacks can be easily rotated under the action of the stress (Figure 9c). Rotations alone do not lead to any increase of the strain. However, they can help the strain accommodation by crystals, as taking place simultaneously with interlamellar shear, interlamellar separation and crystallographic slip processes.

As soon as the elastic deformation is completed some plastic rearrangements of amorphous phase on the microlevel are involved in the process. The plastic deformation of a semicrystalline polymer with a soft amorphous phase ( $T_{\text{def}} > T_g$ ) begins with shape changes of polymer coils and chain fragments in the amorphous phase. Rubbery layers partitioning crystallites are

the most compliant structural regions in the material. Due to low deformation resistance,<sup>[9,35]</sup> they are able to deform already at quite low external stresses, much earlier than any crystallite. However, as deformation advances, the easy path of the free unconstrained deformation in the amorphous phase becomes quickly exhausted, because both amorphous and crystalline components are highly connected and must deform together starting from some low strain level. The chains crossing the crystal-amorphous interfaces, anchored firmly in the crystalline regions, constrain an independent deformation of an amorphous material even at low overall strains. In the amorphous phase, stresses increase quickly with deformation; these stresses transferred to the crystalline phase soon approach the level when the plastic flow of crystallites begins. Crystallites become involved in the plastic flow when the critical resolved shear stress for the easiest slip system is reached. From this point on the plastic deformation of crystallites begins to control the whole deformation kinetics of the sample, while the amorphous layers merely adjust themselves to the deformation of crystalline component. The entire deformation process is reduced then to simultaneous, combined deformation of both components. This control dominates until the breakdown of crystallites.<sup>[19,20,28,31,35]</sup>

Figure 10 shows an evolution of the equivalent stress in crystalline and amorphous components of PE.<sup>[4]</sup> During a deformation the molecular network in the amorphous layers is stretched and chain segments tend to orient themselves in the direction of a maximum extension. As a result the stress needed for further deformation of the network quickly increases. In the range of higher strains the stress increases substantially over the stress related to the deformation of crystalline phase. On the other hand, the slip processes in polymer lamellae are controlled by the nucleation of dislocations and these gliding dislocations are necessarily pushed out of the thin crystal core into the interface, i.e.



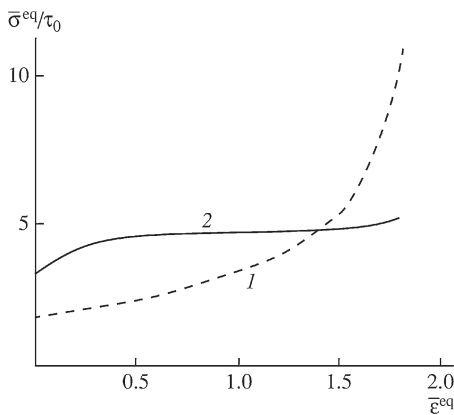


**Figure 10.**

The dependence of normalized equivalent stresses in amorphous (1) and crystalline (2) phases of PE on equivalent strain, under uniaxial compression, Taken from the Ref. [4], with permission of Elsevier, © 1993.

are not trapped in the crystal.<sup>[2]</sup> This property of thin lamellar crystals may explain an important specific feature of deformation – the absence of strain hardening in polymer crystals.<sup>[4,5]</sup> Strain hardening observed macroscopically in a semicrystalline polymer is related rather to the orientational hardening of the amorphous phase and, to a less extent, to reorientation of crystals due to crystal slip (change of the Schmid factor) in later stages of the process.

When the early stages of an independent interlamellar shear are exhausted (by stretching of tie molecules) the crystalline lamellae start to deform along, according to the crystallographic mechanisms. Such a deformation initially proceeds with very little constraints from an amorphous material, which is simply carried along, yet at certain point the deformation of the amorphous phase accompanying deformation of crystallites locks due to an ultimate stretch of tie-molecules, leading to a very high deformation resistance (true strain above  $\epsilon = 1\text{--}1.2$ ,<sup>[28,35]</sup>). At this point a widespread joint structural rearrangements begin. The taut tie-molecules generate stress concentrations on lamellae surfaces, which together with slip instabilities lead to slip localization. As a consequence,

lamellae undergo splitting and heavy fragmentation into blocks, while the interface undergoes intense movements between crystalline and amorphous component. This includes incorporation of some tie-molecules into crystallites (in the form of packing defects) and transfer of some fraction of the crystalline phase into the ordered fraction of the amorphous phase. During such rearrangements the interfaces become diffuse and even may almost dissolve in the highly textured material,<sup>[2,27,109]</sup> while the amorphous phase becomes extremely oriented and ordered. In highly deformed polyethylene by plane-strain compression the crystals produce a sharp single component texture (*‘quasi single crystal’*) while a pseudo-hexagonal packing is developed in the amorphous phase.<sup>[27]</sup> The hexagonal domains become not only well packed and organized in the deformation process but also adjust to the register, which is coherent with the orthorhombic lattice of PE crystallites: (100) planes of hexagonal domains in the amorphous material coincide with (100) planes of orthorhombic crystals. Such very high ordering allows amorphous domains to become capable of transmitting the chain slip from one crystallite to another – dislocations can move from one crystallite to another through the “structured” amorphous phase.<sup>[2,59]</sup>

For an analysis of the macroscopic stress-strain data the deformation behavior of the soft amorphous phase (above  $T_g$ ) can be approximated successfully with simple equations of rubber elasticity, especially in the strain hardening range, where the deformation of crystallites is nearly completed. In such an approach the overall structure of a semicrystalline polymer is considered as consisting of two semi-continuous interpenetrating networks: a skeleton made of crystallites and the molecular network of entangled chains in the amorphous phase.<sup>[19,20]</sup> In modelling of the true stress-true strain curves it is possible then to represent the true stress as a sum of the nearly constant plastic

response of crystallites and the increasing stress related to the deformation of the macromolecular network,<sup>[110-112]</sup> the latter being described by equations of rubber elasticity. Gaussian<sup>[19,20,112,113]</sup> as well as non-Gaussian<sup>[29,30,110,111]</sup> chains were used for that modelling of the stress-strain behavior.

## Deformation Models

Because of the structural and morphological complexity of semicrystalline polymers several models of their plastic deformation were developed in the past to describe the entire deformation sequence. Three of them are mostly discussed at present: the melting-recrystallization model,<sup>[37,38]</sup> the crystallographic model,<sup>[6,8,9,16,35,39]</sup> and the Peterlin's micronecking model.<sup>[33,34,114]</sup>

The melting-recrystallization model and the crystallographic model - discussed in the previous sections - are based on different physical principles. The first of them introduces the concept that yielding and the subsequent plastic flow take place via partial melting of crystallites. It is well known that the initial structure of semicrystalline polymers undergoes significant transformations as a result of deformation. The commonly reported observation that the fibril long period of various semicrystalline polymers plastically drawn far beyond the yield point depends only on the draw temperature,<sup>[33,115]</sup> led a number of authors to hypothesize that the crystalline phase must undergo a strain-induced melting and subsequently recrystallizes during the drawing process, which leads to a new polymer morphology and to the orientation of newly formed crystallites with chains along the direction of the maximum extension. The recrystallization of the molten material and the appearance of a predominant chain orientation reduce the local stress level; this is supposed to be the thermodynamic driving force of the plasticity process. This concept, first formulated by Flory and Yoon,<sup>[37]</sup> more from intuition than from experimental facts, is regularly

taken as a testimony for the phenomenon reality.<sup>[18]</sup> However, the approach as a whole and its basic idea evoke also a serious criticism.<sup>[55,116,117]</sup> Very interesting, critical discussion of the melting-recrystallization model can be found in the recent reviews of Oleinik,<sup>[2]</sup> and Seguela.<sup>[18]</sup>

There were many experimental attempts to prove the correctness of the melting-recrystallization model. The strongest argument in favor of the model is the decrease in the long period as a result of stretching.<sup>[33,115]</sup> Small angle neutron scattering, demonstrating a decreasing ordered cluster size in the deformed samples, was also intensively used to confirm the model.<sup>[118-120]</sup> The arguments however, are not very convincing, because crystallographic models also allow a sufficient number of reasons for a decrease in the crystallite dimensions as a result of the plastic deformation (thinning of crystallites due to slip, loss of thermodynamic stability in thinned crystallites, fracture of lamellae into mosaic blocks),<sup>[2]</sup> A serious flaw of the melting-recrystallization model is its failure to explain the yielding process, even semi-quantitatively. Many present-day results however, convincingly prove that the yielding process in semicrystalline polymers always coexists with crystallographic slip processes in lamellae and the yield stress correlates well with thermal nucleation of dislocation, controlled by the crystal thickness. The results indicate that the plasticity of PE, at least at its early stages, cannot be considered without crystallographic concepts, and so melting is irrelevant here.<sup>[2]</sup> Then, if macroscopic yielding does not begin according to the melting mechanism, only large strains remain for the realization of plastic flow within the framework of the melting concepts. However, there are many processes that occur via fragmentation of crystallites, via their splitting into blocks at large strains, and no melting is required for them. All these processes take place according to mechanisms of the crystallographic origin.<sup>[2]</sup>

There is much published experimental evidence supporting the crystallographic

approach, discussed in previous sections. The directly observed processes of a gradual reorientation of chains during polymer deformation in compression,<sup>[24,25,28,35]</sup> or the results concerning the deformation of *quasi-single crystals* textured samples provide information on the predominant role of crystallographic slip in the PE and PA-6 deformation.<sup>[24,46]</sup> The inter- and intra-crystallite shears observed using various techniques unambiguously confirm the crucial role of crystallographic processes in the plastic deformation of such objects.<sup>[2,6,8,9]</sup>

The model proposed by Peterlin,<sup>[33,34,114]</sup> has a special status today. It undoubtedly remains the most popular model, in spite of its extensive criticism. The pioneer works by Peterlin and coworkers on the large scale plastic deformation of semi-crystalline polymers have led to the elaboration of the first complete model describing the transformation of the original chain-folded lamellar morphology into the partially unfolded-chain fibrillar structure. In that model, the plastic yielding is ascribed to the shearing of the crystalline lamellae followed instantly by their fragmentation into crystal blocks,<sup>[121]</sup> as shown schematically in Figure 11. The model assumes that the transformation of lamellar groups into fibrils during stretching of the initial isotropic spherulitic structure proceeds through formation of numerous ‘micronecks’, which

originate on microcrack boundaries and appear in lamellae during their deformation. In that process folded-chain blocks detach themselves from the lamella, turn with the chain axis in the direction of stretching, and then become incorporated into microfibrils. The resultant fibrils consist of alternating crystalline and amorphous regions.<sup>[33,34]</sup>

The necessary condition for ‘micronecking’ is cavitation, since cavities, which must emerge in the stretched sample remove mechanical constraints on the block rotations. Only cavitations allow a further incorporation of blocks detached from their lamellae into fibrils, as pictured in the model. However, as was demonstrated convincingly, cavitation, being the key stage in the Peterlin’s model is not necessary in other modes of deformation than tensile,<sup>[9,25,28,35]</sup> morphological transformations from initial isotropic structure into microfibrils during plastic deformation can take place also without formation of any cavities or microvoids in the regime of plane-strain or uniaxial compression. In these cavity-free modes the plasticity in lamellae develops according to crystallographic mechanisms, primarily crystallographic chain slip. A multiple repetition and combination of various slip modes leads to a complete transformation of the initial polymer morphology into a new highly oriented structure, and to a new long

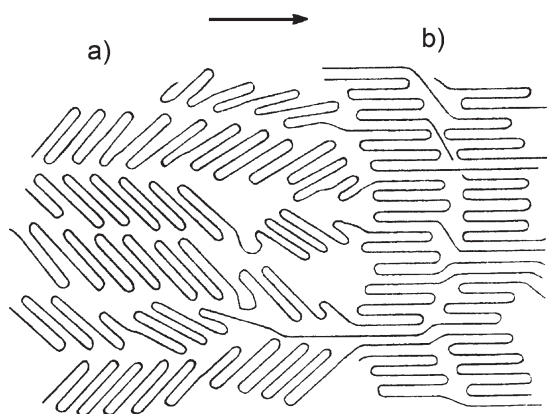


**Figure 11.**

The Peterlin’s model for transformation from lamellar (a) to fibrillar (b) morphology on drawing a semicrystalline polymer. Arrow indicates increasing strain.<sup>[33,34]</sup>

period; all of this taking place without crystallite melting and without cavitation. The initial crystallites undergo a series of continuous crystallographic transformations to reach the final morphology,<sup>[9,25,28,35]</sup> This implies that the model proposed by Peterlin should be revised,<sup>[2,11,35]</sup> It seems that it can describe deformation sequence in tension, yet fails completely when other deformation modes are taken into account. On the other hand, the crystallographic approach can explain the full deformation sequence in any deformation mode, without invoking any catastrophic events like 'micronecking' or melting-recrystallization transformation. Cavitation, if happens in a particular sample or the deformation mode, is merely a side-effect, which seems a non-essential for the plastic deformation process and related transformation of the polymer morphology.<sup>[35]</sup>

Recently, Strobl et al.<sup>[19-23,32,122-125]</sup> focused on the aspects of the deformation of semicrystalline polymers related to the macromolecular network in the amorphous phase. They studied in details the tensile deformation and recovery behavior of several semicrystalline polymers, including PE and found a very interesting and quite simple deformation scheme, which was also found in all other polymers studied. The main feature of this universal behavior is that the process of deformation is controlled by the strain rather than stress. Along the true stress-true strain curves the differential compliance, recovery behavior as well as the crystalline texture change simultaneously at well defined points. Four characteristic transition points were identified and ascribed to activation of various deformation mechanisms,<sup>[19]</sup> The critical strains at which these transitions take place were found nearly invariant over various strain rates and drawing temperatures,<sup>[20,122]</sup> as well as chain architecture or crystallinity of a polymer,<sup>[19,122,124]</sup> In contrast, the corresponding stresses varied significantly with crystallinity as well as with strain rate or temperature of deformation. The invariance of critical strains, i.e. the

strain control of the deformation behavior, implies that the strain can be considered as homogeneous in a semi-crystalline polymer upon its deformation. Active crystallographic slips supported by interlamellar shear modes offer sufficient degrees of freedom to achieve that.<sup>[2,9]</sup>

Upon deformation at temperature above  $T_g$  the load is transmitted by two interpenetrating networks: the skeleton of crystallites and the rubber-like entanglement network of the amorphous regions. However, with an advance of the deformation process, the respective weights change. At low strain, the highly compliant amorphous phase can deform considerably more rapidly than the crystalline phase, yet its contribution to the plastic deformation is limited due to the constraints imposed by adjacent crystals through chains crossing crystal-amorphous interface (tie-molecules, cilia and loose loops, entangled with other chains in the amorphous phase), and its principal role is to transmit load to and between crystalline lamellae,<sup>[2,4,126,127]</sup> However, at high strain the increasing network forces become dominant, which manifests itself in a strong amorphous phase orientation hardening and consequently the macroscopic strain hardening.<sup>[4]</sup> Correspondingly, the yield point (point B of the scheme) is a property of the crystalline skeleton, which above that point is continuously readjusted by operating slip systems. Much more compliant amorphous layers, intimately connected to crystallites follow the changes of crystallites orientation, undergoing interlamellar shear up to the next critical true strain of  $e = 0.6$  (point C), where stresses generated in the stretched network of amorphous chains become high enough to trigger fragmentation of adjacent crystallites,<sup>[19]</sup> Finally, at high strains (point D,  $e = 1$ ), deformation behavior becomes dominated by forces produced by the stretched entanglement network of the amorphous phase.

Studies of high strain deformation and recovery behavior of other polymers such as PET, PBT or Nylon-6,<sup>[128-133]</sup> generally confirmed the deformations scheme

proposed by Strobl. Moreover, the studies of a broad range of polyethylenes deformed in compression by Bartczak et al.<sup>[28-31,134]</sup> demonstrated that the Strobl's scheme is valid not only in the tensile but also in compression deformation mode and can be considered as an universal deformation scheme. This scheme, proposed by Strobl et al.<sup>[19]</sup> and refined by Bartczak,<sup>[31]</sup> consisting of 4 characteristic points of nearly invariant strain can be summarized as follows (cf. Figure 12):

- (A) the end of the elastic proportionality range; the onset of isolated inter- and intralamellar slip processes (true strain,  $e \sim 0.02$ ),
- (B) a merge of local slip events into a widespread, collective activity of crystallographic slips and interlamellar shear; macroscopic yield point is reached ( $e \sim 0.1$ )
- (C) exhaustion and a temporary lock of the shear of amorphous layers due to full straining of tie-molecules, which causes some stress concentration in lamellae, resulting in the slip localization and lamellae cooperative bending, kinking and/or limited fragmentation. This releases partially the constraints imposed on amorphous phase and restores its deformability along an easy deformation path at low stress ( $e \sim 0.6$ )
- (D) the second lock of the shear of amorphous layers due to full stretch of the molecular network. Corresponding stress increase leads to a massive fragmentation of lamellar crystals into small blocks due to severe slip localization (slip instability) in lamellae already thinned substantially by advanced fine slip. This fragmentation releases constraints, which in turn allows rotations and restructurization of highly sheared crystal blocks, resulting in appearance of a new long period in the direction of extension (formation of the final fibrillar structure). Strong orientation hardening of the amorphous phase brings an onset of chain disentangle-

ments, leading to partial destruction of the molecular network ( $e \sim 0.9-1.2$ , depending on the molecular network density).

Experimental evidence demonstrated that the origin of the transformation at the true strain near  $e = 0.6$  (point C) is the exhaustion and locking of the interlamellar shear of the amorphous layers due to ultimate extension of tie molecules. This leads to stress build-up and consequently to localization of crystallographic slip (stress concentrations at interfaces around points of tie-molecules entrance into lamella), which results in a limited destruction of the lamellar structure. While in the less constrained conditions of the tensile deformation this process actually leads to a widespread destruction of the existing lamellar structure and formation of microfibrils, in compression experiments, where much stronger deformation constraints are present, it results merely in a very limited lamella fragmentation mostly by cooperative kinking of stacked lamellae (see Figures 5 and 13). In both cases however, fragmentation and subsequent rotations of crystals bring a partial release of constraints in amorphous layers, which allows further deformation of both crystalline and amorphous material along a relative easy

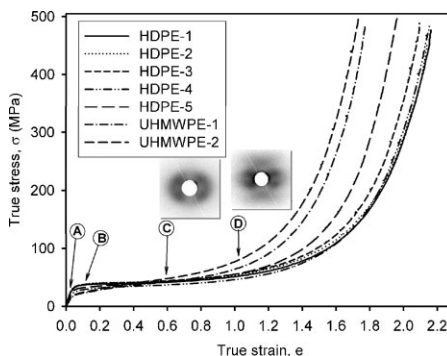


**Figure 12.**

The true stress-true strain curves of PE samples of various molecular mass deformed in the plane strain compression with 4 critical points marked. Insets show 2D-SAXS patterns obtained for HDPE-1 at point C (lamella kinking) and D (fragmentation and restructurization).<sup>[28,30,31]</sup>

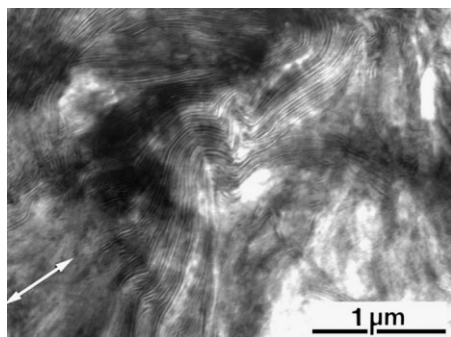


**Figure 13.**

TEM micrograph of ultra-thin section of PE deformed to the true strain of  $e = 0.8$ . Arrow indicates the direction of compression loading (LD). Direction of flow is perpendicular to LD in the plane of section. Reproduced from the Ref. [31] with permission of Elsevier © 2005

deformation path, without much stress built-up.

A more advanced destruction of lamellar structure can happen in compression later, at higher compressive strains, well above  $e = 1$ , although only in samples of relatively low molecular mass or at high deformation temperature.<sup>[28,31]</sup> Samples of higher molecular mass do not undergo such an intense process of lamellae fragmentation in compression at room temperature

even at high strain. Both lamellar kinks or more advanced, heavy destruction of lamellar structure lead to a substantial reorientation of crystallites to favor further advance of chain slips as well as to some modification of the topology of the entangled network in adjacent amorphous layers, which relieves temporarily some of the deformation constraints. The transformation replacing initial lamellae with the new structure is shown schematically in Figure 14. All these phenomena allow for further accommodation of the strain by chain slip in the crystalline lamellae and accompanying shear of interlamellar amorphous layers, although the stress increases substantially due to orientation hardening of the amorphous phase.

To produce a truly irreversible deformation of a semicrystalline polyethylene it is necessary to deform it to the strain of at least  $e = 1.0$  (point D of the deformation scheme). Up to this point, nearly all strain related to the deformation of amorphous part can be recovered either by prolonged storage or annealing at high temperature. However, with an increasing strain the stress generated by stretching the entanglement network becomes high enough to modify or partially destroy that network.

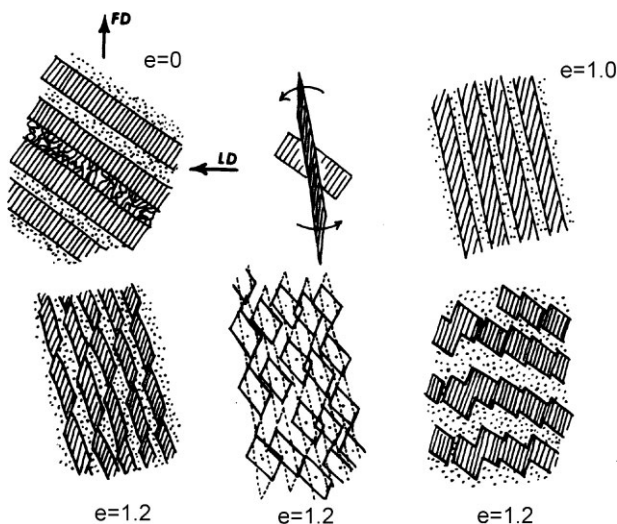


**Figure 14.**

Sketch of the process of lamellae fragmentation at the strain around  $e = 1 - 1.2$ , leading to formation of new long period. Drawn after the Ref. [35] with permission of ACS © 1992.



Consequently, at the strain of above  $e = 1.0$ – $1.2$  a gradual dissolution of the network by chain disentanglements sets in. This leads to a permanent, totally irreversible plastic flow of the amorphous component in addition to the irreversible plastic deformation of the crystalline component and consequently to the erasure of the ‘memory’ of the undeformed macro-state of the material.

That universal deformation scheme, outlined above, relies on deformation micromechanisms which are predominantly of crystallographic nature. Plastic deformation starts at the yield point with widespread crystal slip processes, supported by interlamellar slip in the amorphous component. Occasionally, twinning modes and martensitic transformations are engaged.<sup>[24,25,35]</sup> Also other phenomena, occurring at larger strains are closely related to the crystallographic mechanisms, e.g. fragmentation of lamellae results from a heavy localization of the slip process and its change from fine to coarse mode. The discussed scheme shows additionally quite clearly the deep mutual influence and cooperative deformation of both crystalline and amorphous components. This cooperation is the primary source of exceptional ductility of semicrystalline polymers. The obtained results demonstrates clearly that the cavitation, necessary in the Peterlin’s model, is really unessential in producing high deformation and appearance of the final highly oriented structure. This can be effectively accomplished with only crystallographic mechanisms employed. Cavitation happens only in the less constrained deformation modes, as uniaxial tension. In such a case, it makes easier the final transformation to fibrillar structure, yet this can be achieved also in cavity-free modes (although a higher stress is then generated). It should also be noted, that crystallographic mechanisms lead to thinning of lamellae (fine slip), their fragmentation into blocks, and consequently can result in a reduction of the crystallinity of the deformed material.<sup>[2,6,8,9,35]</sup> This means that the initial

crystallites in the deformed material can become defective and sometimes even completely disappear (when the block size is reduced to the critical one and the crystallite becomes thermodynamically unstable). These features, surely related to crystallographic mechanisms, are actually the same as those used to support a melting-recrystallization model.

## Conclusion

The progress in research of the deformation of semicrystalline polymers achieved in last years allowed better understanding of this process. It is now very well established that the plastic deformation of a semicrystalline polymer is a complex series of continuous processes, that involve several mechanisms, mostly of crystallographic nature. Studies on plastic deformation in cavity-free modes demonstrated clearly that any discontinuous, “catastrophic” process is not necessary to achieve large strains. That finding is opposite to the “micronecking” model proposed long time ago by Peterlin.

The most important mechanism of plastic deformation of crystalline phase is the chain slip, supported by transverse slip and in some polymers by twinning and/or stress induced martensitic transformations. A very important role in the deformation sequence is played by the partially reversible shear deformation of amorphous interlamellar layers, producing not only high orientation of amorphous component but also influencing deeply the deformation of crystalline phase, since both phases are strongly connected and must deform simultaneously and consistently.

[1] A. Keller, *Rep Prog Phys* **1968**, 31, 623–704.

[2] E. F. Oleinik, *Polymer Science C* **2003**, 45, 17–117.

[3] C. Thomas, V. Ferreiro, G. Coulon, R. Seguela, *Polymer* **2007**, 48, 6041–6048.

[4] B. J. Lee, A. S. Argon, D. M. Parks, S. Ahzi, Z. Bartczak, *Polymer* **1993**, 34, 3555–3575.

- [5] B. J. Lee, A. S. Argon, S. Ahzi, *J Mech Phys Solids* **1993**, 41, 1651-1687.
- [6] P. B. Bowden, R. J. Young, *J Mater Sci* **1974**, 9, 2034-2051.
- [7] R. J. Young, In *Developments in Polymer Fracture-1*, E. H. Andrews, Ed.; Applied Science, London **1979**, p 223-261.
- [8] J.-M. Haudin, In *Plastic Deformation of Amorphous and Semicrystalline Materials*, B. Escaig, C. G'Sell, Eds.; Les Ulis: Les Éditions de Physique, Paris **1982**, p 291-311.
- [9] L. Lin, A. S. Argon, *J Mater Sci* **1994**, 29, 294-323.
- [10] R. Porter, L.-H. Wang, *Rev Macromol ChemPhys* **1995**, 35, 63.
- [11] E. F. Oleinik, S. N. Rudnev, O. B. Salamatina, *Polymer Science A* **2007**, 49, 1302-1327.
- [12] A. Galeski, G. Regnier, In *Nano- and Micromechanics of Polymer Blends and Composites*, J. Karger-Kocsis, S. Fakirov, Eds.; Hanser Publishers, Munich **2009**, p 3-58.
- [13] B. Lotz, J.-C. Wittman, In *Material Science and Technology A Comprehensive Treatment*, E. L. Thomas, Ed.; VCH, New York **1993**, p 79-152.
- [14] P. J. Barham, In *Material Science and Technology A Comprehensive Treatment*, E. L. Thomas, Ed.; VCH, New York **1993**, p 153-212.
- [15] B. Crist, In *Material Science and Technology A Comprehensive Treatment*, E. L. Thomas, Ed.; VCH, New York **1993**, p 427-470.
- [16] R. Seguela, *Journal of Polymer Science Part B-Polymer Physics* **2002**, 40, 593-601.
- [17] R. Seguela, *Journal of Polymer Science Part B-Polymer Physics* **2005**, 43, 1729-1748.
- [18] R. Seguela, *e-Polymers* **2007**, 032, 1-20.
- [19] R. Hiss, S. Hobeika, C. Lynn, G. Strobl, *Macromolecules* **1999**, 32, 4390-4403.
- [20] S. Hobeika, Y. Men, G. Strobl, *Macromolecules* **2000**, 33, 1827-1833.
- [21] K. Hong, A. Rastogi, G. Strobl, *Macromolecules* **2004**, 37, 10165-10173.
- [22] K. Hong, A. Rastogi, G. Strobl, *Macromolecules* **2004**, 37, 10174-10179.
- [23] K. Hong, G. Strobl, *Macromolecules* **2006**, 39, 268-273.
- [24] Z. Bartczak, A. S. Argon, R. E. Cohen, *Macromolecules* **1992**, 25, 5036-5053.
- [25] Z. Bartczak, R. E. Cohen, A. S. Argon, *Macromolecules* **1992**, 25, 4692-4704.
- [26] Z. Bartczak, A. S. Argon, R. E. Cohen, *Polymer* **1994**, 35, 3427-3441.
- [27] Z. Bartczak, A. Galeski, A. S. Argon, R. E. Cohen, *Polymer* **1996**, 37, 2113-2123.
- [28] Z. Bartczak, E. Lezak, *Polymer* **2005**, 46, 6050-6063.
- [29] Z. Bartczak, *Macromolecules* **2005**, 38, 7702-7713.
- [30] Z. Bartczak, M. Kozanecki, *Polymer* **2005**, 46, 8210-8221.
- [31] Z. Bartczak, *Polymer* **2005**, 46, 10339-10354.
- [32] B. Na, Q. Zhang, Q. Fu, Y. Men, K. Hong, G. Strobl, *Macromolecules* **2006**, 39, 2584-2591.
- [33] A. Peterlin, In *Encyclopedia of Polymer Science and Engineering*, H. F. Mark, N. M. Bikales, C. G. Overberger, G. Menges, J. I. Kroschwitz, Eds.; Wiley **1987**, p 72-94.
- [34] A. Peterlin, *Plastic Deformation of Polymers*, Marcel Dekker, New York **1971**.
- [35] A. Galeski, Z. Bartczak, A. S. Argon, R. E. Cohen, *Macromolecules* **1992**, 25, 5705-5718.
- [36] R. J. Samuels, *Structured Polymer Properties*, Wiley, New York **1974**.
- [37] P. J. Flory, D. Y. Yoon, *Nature* **1978**, 272, 226-229.
- [38] A. N. Gent, S. Madan, *Journal of Polymer Science Part B-Polymer Physics* **1989**, 27, 1529-1542.
- [39] R. J. Young, *Philos Mag* **1976**, 30, 86-94.
- [40] I. L. Hay, A. Keller, Z. Z. Kolloid, *Polym* **1965**, 204, 43-74.
- [41] H. Gleiter, A. S. Argon, *Philos Mag* **1971**, 24, 71-80.
- [42] D. Lewis, E. J. Whiller, W. F. Maddams, J. E. Preedy, *Journal of Polymer Science Part A-2: Polymer Physics* **1972**, 10, 369-373.
- [43] R. J. Young, P. B. Bowden, J. Ritchie, J. G. Rider, *Journal of Material Science* **1973**, 8, 23-36.
- [44] A. Galeski, *Progress in Polymer Science* **2003**, 28, 1643-1699.
- [45] E. Schmid, W. Boas, *Plasticity of Crystals*, Hughes, London **1950**.
- [46] L. Lin, A. S. Argon, *Macromolecules* **1992**, 25, 4011-4024.
- [47] A. Keller, J. G. Rider, *Journal of Material Science* **1966**, 1, 389-398.
- [48] T. Hinton, J. G. Rider, *Journal of Applied Physics* **1968**, 39, 4932-4937.
- [49] P. B. Bowden, R. J. Young, *Nature* **1971**, 229, 23-25.
- [50] D. Shinozaki, G. Groves, *Journal of Material Science* **1973**, 8, 71-78.
- [51] R. M. Caddell, R. S. Raghava, A. G. Atkins, *Journal of Material Science* **1973**, 8, 1641-1646.
- [52] Z. Bartczak, A. Galeski, *Polymer* **1999**, 40, 3677-3684.
- [53] C. G'Sell, J.-M. Haudin, *Introduction: a la mécanique des polymères*, INPL-MECAMJT-APPOLIOR-FIRTECH, Nancy **1993**.
- [54] R. S. Porter, *Polymer Preprints* **1971**, 12, 39.
- [55] R. Seguela, S. Elkoun, V. Gaucher-Miri, *Journal of Material Science* **1998**, 33, 1801-1807.
- [56] I. L. Hay, A. Keller, *Journal of Polymer Science Part C: Polymer Symposia* **1970**, 30, 289-295.
- [57] R. E. Robertson, *Journal of Polymer Science Part A-2: Polymer Physics* **1971**, 9, 1255-1269.
- [58] S. G. Burnay, G. W. Groves, *Journal of Material Science* **1978**, 13, 639-646.
- [59] L. Lin, A. S. Argon, *Macromolecules* **1994**, 27, 6903-6914.
- [60] A. Bellare, A. S. Argon, R. E. Cohen, *Polymer* **1993**, 34, 1393-1403.

- [61] D. M. Parks, S. Ahzi, *J Mech Phys Solids* **1990**, 38, 701-724.
- [62] F. C. Frank, A. Keller, A. O'Connor, *Philos Mag* **1958**, 3, 64-74.
- [63] H. Kiho, A. Peterlin, P. H. Geil, *Journal of Applied Physics* **1964**, 35, 1599-1605.
- [64] P. Allan, E. B. Crellin, M. Bevis, *Philos Mag* **1973**, 27, 127-145.
- [65] M. F. Butler, A. M. Donald, W. Bras, G. R. Mant, G. E. Derbyshire, A. J. Ryan, *Macromolecules* **1995**, 28, 6383-6393.
- [66] M. F. Butler, A. M. Donald, A. J. Ryan, *Polymer* **1997**, 38, 5521-5538.
- [67] M. F. Butler, A. M. Donald, *Macromolecules* **1998**, 31, 6234-6249.
- [68] M. F. Butler, A. M. Donald, A. J. Ryan, *Polymer* **1998**, 39, 39-52.
- [69] W. Wu, A. S. Argon, A. P. L. Turner, *Journal of Polymer Science: Polymer Physics Edition* **1972**, 10, 2397-2407.
- [70] M. Bevis, E. B. Crellin, *Polymer* **1971**, 12, 666-684.
- [71] P. H. Geil, *Polymer Single Crystals*, Interscience, New York **1961**.
- [72] B. Wunderlich, *Macromolecular Physics, Crystal Structure, Morphology, Defects*, Academic Press, New York **1973**.
- [73] H. D. Keith, W. Y. Chen, *Polymer* **2002**, 43, 6263-6272.
- [74] A. W. Agar, F. C. Frank, A. Keller, *Philos Mag* **1959**, 4, 32-55.
- [75] J. Petermann, H. Gleiter, *Philos Mag* **1972**, 25, 813-816.
- [76] J. Petermann, R. M. Gohil, *Journal of Material Science* **1973**, 8, 673-675.
- [77] J. M. Peterson, *Journal of Applied Physics* **1966**, 37, 4047-4050.
- [78] J. M. Peterson, *Journal of Applied Physics* **1968**, 39, 4920-4928.
- [79] L. G. Shadrake, F. Guiu, *Philos Mag* **1976**, 34, 565-581.
- [80] R. J. Young, *Material Forum* **1988**, 11, 210-216.
- [81] B. Crist, C. J. Fisher, P. Howard, *Macromolecules* **1989**, 22, 1709-1718.
- [82] O. Darras, R. Seguela, *Journal of Polymer Science Part B: Polymer Physics* **1993**, 31, 759-766.
- [83] W. J. O'Kane, R. J. Young, A. J. Ryan, *Journal of Macromolecular Science - Physics* **1995**, 34, 427-458.
- [84] L. G. Shadrake, F. Guiu, *Philos Mag* **1979**, 39, 785-796.
- [85] D. J. Bacon, K. Tharmalingam, *Journal of Material Science* **1983**, 18, 884-893.
- [86] R. J. Young, *Philos Mag* **1974**, 30, 85-94.
- [87] T. Kazmierczak, A. Galeski, A. S. Argon, *Polymer* **2005**, 46, 8926-8936.
- [88] A. S. Argon, A. Galeski, T. Kazmierczak, *Polymer* **2005**, 46, 11798-11805.
- [89] R. Peierls, *Proc Phys Soc* **1940**, 289, 34-37.
- [90] F. R. N. Nabarro, *Proc Phys Soc* **1947**, 59, 256-272.
- [91] A. J. Peacock, L. Mandelkern, R. G. Alamo, J. G. Fatou, *Journal of Material Science* **1998**, 33, 2255-2268.
- [92] R. W. K. Honeycomb, *The Plastic Deformation of Metals*, Edward Arnold Ltd, London **1968**.
- [93] B. Crist, *Polymer Communications* **1989**, 30, 69-71.
- [94] N. W. J. Brooks, R. A. Duckett, I. M. Ward, *Journal of Polymer Science part B Polymer Physics Edition* **1998**, 36, 2177-2189.
- [95] R. Seguela, *Journal of Polymer Science part B Polymer Physics Edition* **2002**, 40, 593-601.
- [96] N. W. J. Brooks, M. Mukhtar, *Polymer* **2000**, 41, 1475-1480.
- [97] G. Xu, A. S. Argon, M. Ortiz, *Philos Mag* **1995**, A72, 415-451.
- [98] G. Xu, A. S. Argon, M. Ortiz, *Philos Mag* **1997**, A75, 341-367.
- [99] G. Xu, C. Zhang, *J Mech Phys Solids* **2003**, 51, 1371-1394.
- [100] G. Xu, *Philos Mag* **2002**, A82, 3177-3185.
- [101] J. A. W. van Dommelen, D. M. Parks, M. C. Boyce, W. A. M. Brekelmans, F. P. T. Baaijens, *Polymer* **2003**, 44, 6089-6101.
- [102] J. A. W. van Dommelen, D. M. Parks, M. C. Boyce, W. A. M. Brekelmans, F. P. T. Baaijens, *J Mech Phys Solids* **2003**, 51, 519-541.
- [103] A. Cowking, J. G. Rider, I. L. Hay, A. Keller, *Journal of Material Science* **1968**, 3, 646-654.
- [104] A. Cowking, J. G. Rider, *Journal of Material Science* **1969**, 4, 1051-1058.
- [105] A. Keller, D. P. Pope, *Journal of Material Science* **1971**, 6, 453-478.
- [106] A. Pawlak, A. Galeski, *Macromolecules* **2005**, 38, 9688-9697.
- [107] C. A. Garber, E. S. Clark, *Journal of Macromolecular Science Part B Physics* **1970**, 4, 499-517.
- [108] M. Krumova, S. Hennig, G. H. Michler, *Philos Mag* **2006**, 86, 1689-1712.
- [109] H. Schonherr, G. J. Vancso, A. S. Argon, *Polymer* **1995**, 36, 2115-2121.
- [110] R. N. Haward, *Polymer* **1999**, 5821-5832.
- [111] R. N. Haward, *Journal of Polymer Science Part B: Polymer Physics* **2007**, 45, 1090-1099.
- [112] R. N. Haward, G. Thackray, *Proc R Soc London Ser A* **1967**, 302, 453-472.
- [113] B. A. G. Schrauwen, R. P. M. Janssen, L. E. Govaert, H. E. H. Meijer, *Macromolecules* **2004**, 37, 6069-6078.
- [114] A. Peterlin, *Journal of Material Science* **1971**, 6, 490-508.
- [115] R. Popli, L. Mandelkern, *Journal of Polymer Science Part B: Polymer Physics* **1987**, 25, 441-483.
- [116] V. Gaucher-Miri, P. Francois, R. Seguela, *Macromolecules* **1997**, 30, 1158-1167.
- [117] V. Gaucher-Miri, S. Elkoun, R. Seguela, *Polymer Engineering & Science* **1997**, 37, 1672-1683.
- [118] H. H. Chuah, J. S. Lin, R. S. Porter, *Macromolecules* **1986**, 19, 2732-2736.
- [119] W. Wu, G. D. Wignall, L. Mandelkern, *Polymer* **1992**, 33, 4137-4140.

- [120] R. G. Alamo, L. Mandelkern, B. K. Annis, J. Strizak, G. D. Wignall, *Polymer* **1996**, 37, 137–140.
- [121] A. Peterlin, *Journal of Polymer Science Part C: Polymer Symposia* **1965**, 9, 61–89.
- [122] Y. Men, G. Strobl, *Journal of Macromolecular Science - Physics* **2001**, B40, 775–796.
- [123] M. Al-Hussein, G. Strobl, *Macromolecules* **2002**, 35, 8515–8520.
- [124] Q. Fu, Y. Men, G. Strobl, *Polymer* **2003**, 44, 1927–1933.
- [125] Q. Fu, Y. Men, G. Strobl, *Polymer* **2003**, 44, 1941–1947.
- [126] N. Brown, I. M. Ward, *Journal of Material Science* **1983**, 18, 1405–1420.
- [127] R. Seguela, O. Darras, *Journal of Material Science* **1994**, 29, 5342–5347.
- [128] J. B. Park, D. R. Uhlmann, *Journal of Applied Physics* **1973**, 42, 3800–3805.
- [129] J. B. Park, D. R. Uhlmann, *Journal of Applied Physics* **1973**, 44, 201–206.
- [130] N. Tanaka, *Journal of Thermal Analysis* **1996**, 46, 1021–1031.
- [131] P. Charoensirisomboon, H. Saito, T. Inoue, Y. Oishi, K. Mori, *Polymer* **1998**, 39, 2089–2093.
- [132] A. Pegoretti, A. Guardini, C. Migliaresi, T. Ricco, *Polymer* **2000**, 41, 1857–1864.
- [133] A. Pegoretti, A. Guardini, C. Migliaresi, T. Ricco, *Journal of Applied Polymers Science* **2000**, 78, 1664–1770.
- [134] E. Lezak, Z. Bartczak, *Journal of Applied Polymer Science* **2007**, 105, 14–24.